

3D generalized nonhyperboloidal moveout approximation

Yanadet Sripanich¹, Sergey Fomel¹, Alexey Stovas², and Qi Hao²

ABSTRACT

Moveout approximations are commonly used in velocity analysis and time-domain seismic imaging. We revisit the previously proposed generalized nonhyperbolic moveout approximation and develop its extension to the 3D multi-azimuth case. The advantages of the generalized moveout approximation are its high accuracy and its ability to reduce to several other known approximations with particular choices of parameters. The proposed 3D functional form involves 17 independent parameters instead of five as in the 2D case. These parameters can be defined by zero-offset traveltimes and four additional far-offset rays. In our tests, the proposed approximation achieves significantly higher accuracy than previously proposed 3D approximations.

INTRODUCTION

Reflection moveout approximation is an important ingredient for velocity analysis and other time-domain processing techniques (Yilmaz, 2001). As a function of the source-receiver offset, the two-way reflection traveltimes has the well-known hyperbolic expression, which is exact for plane reflectors in homogeneous isotropic or elliptically anisotropic overburden and approximately valid for small offsets in other cases. This behavior is generally valid for any pure-mode reflections thanks to the source-receiver reciprocity (Thomsen, 2014). At larger offsets, moveout may deviate from hyperbola and behave nonhyperbolically due to the effects of either anisotropy or heterogeneity (Fomel and Grechka, 2001).

In 2D, many extended moveout approximations have been proposed and are designed to work with large-offset seismic data. They have led to better stacked sections and successful inversions for

anisotropic parameters (Hake et al., 1984; Castle, 1994; Tsvankin and Thomsen, 1994; Alkhalifah and Tsvankin, 1995; Alkhalifah, 1998; Pech et al., 2003; Fomel, 2004; Taner et al., 2005; Ursin and Stovas, 2006; Blas, 2009; Aleixo and Schleicher, 2010; Golkov and Stovas, 2012; Blas, 2013). Fomel and Stovas (2010) propose an approximation, which includes five independent parameters that can be defined from traveltimes derivatives with respect to the offset at the zero-offset ray and one far-offset ray. This approximation was named the generalized moveout approximation (GMA) because its functional form reduces to several other known approximation forms with particular choices of parameters, and thus it provides a systematic view on the effect of various choices of parameters on the approximation accuracy. Its application to homogeneous transversely isotropic (TI) media is studied by Stovas (2010), and the GMA analog in the τ - p domain is developed by Stovas and Fomel (2012). The case of P-SV waves in horizontally layered transversely isotropic media with vertical symmetry axis (VTI) media is investigated by Hao and Stovas (2015).

The most basic expression for a 3D moveout approximation that works in arbitrary anisotropic heterogeneous media with small offsets can be expressed as the normal moveout (NMO) ellipse, and it originates in the second-order Taylor polynomial of traveltimes squared around the zero offset (Grechka and Tsvankin, 1998; Tsvankin and Grechka, 2011). Several large-offset 3D moveout approximations have also been proposed and applied to seismic velocity analysis in azimuthally anisotropic media (Al-Dajani and Tsvankin, 1998; Al-Dajani et al., 1998; Pech and Tsvankin, 2004; Xu et al., 2005; Grechka and Pech, 2006; Vasconcelos and Tsvankin, 2006; Farra et al., 2016). The general expression for the quartic coefficients is studied by Fomel (1994) and Pech et al. (2003) based on an extension of the normal-incident-point theorem.

In this paper, we revisit the 2D generalized nonhyperbolic moveout approximation and develop its natural extension to 3D. We subsequently show that the proposed approximation can be reduced to other known forms with different choices of parameters. Using numerical tests, we show that the 3D GMA can be several orders of magnitude more accurate than previously proposed 3D moveout

Manuscript received by the Editor 4 April 2016; revised manuscript received 15 September 2016; published online 24 January 2017.

¹The University of Texas, Bureau of Economic Geology, John A. and Katherine G. Jackson School of Geosciences, Austin, Texas, USA. E-mail: sripanichy@utexas.edu; sergey.fomel@beg.utexas.edu.

²Norwegian University of Science and Technology (NTNU), Trondheim, Norway. E-mail: alexey.stovas@ntnu.no; qi.hao@ntnu.no.

© 2017 Society of Exploration Geophysicists. All rights reserved.

approximations, at the expense of increasing the number of adjustable parameters. The accuracy and analytical properties of the proposed approximation make it an appropriate choice for 3D moveout approximation in the case of long-offset seismic data.

NONHYPERBOLOIDAL MOVEOUT APPROXIMATION

Let $t(x, y)$ represent the two-way reflection traveltimes as a function of the source-receiver offset with components x and y in a given acquisition coordinate frame. We propose the following general functional form of nonhyperboloidal moveout approximation (Sripanich and Fomel, 2015a):

$$t^2(x, y) \approx t_0^2 + W(x, y) + \frac{A(x, y)}{t_0^2 + B(x, y) + \sqrt{t_0^4 + 2t_0^2B(x, y) + C(x, y)}}, \quad (1)$$

where

$$\begin{aligned} W(x, y) &= W_1x^2 + W_2xy + W_3y^2, \\ A(x, y) &= A_1x^4 + A_2x^3y + A_3x^2y^2 + A_4xy^3 + A_5y^4, \\ B(x, y) &= B_1x^2 + B_2xy + B_3y^2, \\ C(x, y) &= C_1x^4 + C_2x^3y + C_3x^2y^2 + C_4xy^3 + C_5y^4, \end{aligned} \quad (2)$$

and t_0 denotes the two-way traveltime at the zero offset. The total number of independent parameters in equation 1 is 17, including t_0 , W_i , A_i , B_i , and C_i . Simple algebraic transformation of equation 1 leads to the following expression in polar coordinates:

$$t^2(r, \alpha) \approx t_0^2 + W_r(\alpha)r^2 + \frac{A_r(\alpha)r^4}{t_0^2 + B_r(\alpha)r^2 + \sqrt{t_0^4 + 2t_0^2B_r(\alpha)r^2 + C_r(\alpha)r^4}}, \quad (3)$$

where

$$\begin{aligned} W_r(\alpha) &= (1/V_{\text{NMO}}^2(\alpha)) = W_1 \cos^2 \alpha + W_2 \cos \alpha \sin \alpha \\ &\quad + W_3 \sin^2 \alpha, \\ A_r(\alpha) &= A_1 \cos^4 \alpha + A_2 \cos^3 \alpha \sin \alpha + A_3 \cos^2 \alpha \sin^2 \alpha \\ &\quad + A_4 \cos \alpha \sin^3 \alpha + A_5 \sin^4 \alpha, \\ B_r(\alpha) &= B_1 \cos^2 \alpha + B_2 \cos \alpha \sin \alpha + B_3 \sin^2 \alpha, \\ C_r(\alpha) &= C_1 \cos^4 \alpha + C_2 \cos^3 \alpha \sin \alpha + C_3 \cos^2 \alpha \sin^2 \alpha \\ &\quad + C_4 \cos \alpha \sin^3 \alpha + C_5 \sin^4 \alpha, \end{aligned} \quad (4)$$

$r = \sqrt{x^2 + y^2}$ represents the absolute offset, and α denotes the azimuthal angle from the x -axis. Along a fixed azimuth α , equation 1 reduces to the generalized nonhyperbolic moveout approximation of Fomel and Stovas (2010).

Connections with other approximations

- 1) Setting $A_i = 0$, we can obtain the expression of NMO ellipse from equation 1 (Grechka and Tsvankin, 1998):

$$t^2(x, y) \approx t_0^2 + W(x, y). \quad (5)$$

- 2) Setting $C_1 = B_1^2$, $C_2 = 2B_1B_2$, $C_3 = 2B_1B_3 + B_2^2$, $C_4 = 2B_2B_3$, and $C_5 = B_3^2$, we can reduce equation 1 to the following rational approximation, which is reminiscent of several previously proposed approximations (Tsvankin and Thomsen, 1994; Ursin and Stovas, 2006):

$$t^2(x, y) \approx t_0^2 + W(x, y) + \frac{A(x, y)}{2(t_0^2 + B(x, y))}. \quad (6)$$

- 3) Considering equation 3 and a horizontal orthorhombic model with $A_1 = -4\eta_2 W_1^2$, $A_3 = -4\eta_{xy} W_1 W_3$, $A_5 = -4\eta_1 W_3^2$, $A_2 = A_4 = 0$, $B_i = 0$, and $C_i = 0$, where η_{xy} is given by Stovas (2015):

$$\eta_{xy} = \sqrt{\frac{(1 + 2\eta_1)(1 + 2\eta_2)}{1 + 2\eta_3}} - 1, \quad (7)$$

equation 3 reduces to the quartic approximation under the acoustic approximation (Alkhalifah, 2003) without the long-offset normalization:

$$\begin{aligned} t^2(r, \alpha) &\approx t_0^2 + W_r(\alpha)r^2 + A_r(\alpha)r^4 \\ &\approx t_0^2 + W_r(\alpha)r^2 - \frac{2}{t_0^2} (\eta_2 W_1^2 \cos^4 \alpha \\ &\quad + \eta_{xy} W_1 W_3 \cos^2 \alpha \sin^2 \alpha + \eta_1 W_3^2 \sin^4 \alpha)r^4, \end{aligned} \quad (8)$$

where, η_1 , η_2 , and η_3 represent the anellipticity parameters in the planes $[y, z]$, $[x, z]$, and $[x, y]$, respectively (Alkhalifah and Tsvankin, 1995; Alkhalifah, 2003; Stovas, 2015), and their definitions in terms of stiffness coefficients under the Voigt notation can be given as follows:

$$\eta_1 = \frac{c_{22}(c_{33} - c_{44})}{2c_{23}(c_{23} + 2c_{44}) + 2c_{33}c_{44}} - \frac{1}{2}, \quad (9)$$

$$\eta_2 = \frac{c_{11}(c_{33} - c_{55})}{2c_{13}(c_{13} + 2c_{55}) + 2c_{33}c_{55}} - \frac{1}{2}, \quad (10)$$

$$\eta_3 = \frac{c_{22}(c_{11} - c_{66})}{2c_{12}(c_{12} + 2c_{66}) + 2c_{11}c_{66}} - \frac{1}{2}. \quad (11)$$

The approximation proposed by Al-Dajani and Tsvankin (1998) and Al-Dajani et al. (1998) has the following additional long-offset normalization factor on the quartic term:

$$1 + A_r^*(\alpha)r^2, \quad (12)$$

where $A_r^*(\alpha) = A_r(\alpha)/(1/V_{\text{hor}}^2(\alpha) - 1/V_{\text{NMO}}^2(\alpha))$ and $V_{\text{hor}}(\alpha)$ is the phase velocity of P-waves in the $[x, y]$ plane as opposed to the group velocity. This introduction of the normalization term leads to

$$t^2(r, \alpha) \approx t_0^2 + W_r(\alpha)r^2 + \frac{A_r(\alpha)}{1 + A_r^*(\alpha)r^2}r^4. \quad (13)$$

In the limit of $V_{\text{NMO}}^2 \rightarrow V_{\text{hor}}^2$, $A_r^*(\alpha) \rightarrow 0$ and the normalization term becomes equal to one.

- 4) In an alternative approach to parameterization in an orthorhombic model, we consider the rational approximation in equation 6 with A_i and B_i normalized by a factor of $1/V_{\text{NMO}}^2(\alpha)$. Under the choice of linearized coefficients $A_r(\alpha) = -4\eta(\alpha)/V_{\text{NMO}}^4(\alpha)$ and $B_r(\alpha) = (1 + 2\eta(\alpha))/V_{\text{NMO}}^2(\alpha)$, this leads to the moveout approximation of the form proposed by Xu et al. (2005) and Vasconcelos and Tsvankin (2006):

$$\begin{aligned} t^2(r, \alpha) \approx t_0^2 + W_r(\alpha)r^2 \\ - \frac{2\eta(\alpha)}{V_{\text{NMO}}^2(\alpha)[t_0^2 V_{\text{NMO}}^2(\alpha) + (1 + 2\eta(\alpha))r^2]} r^4, \end{aligned} \quad (14)$$

where

$$\eta(\alpha) = \eta_2 \cos^2 \alpha - \eta_3 \cos^2 \alpha \sin^2 \alpha + \eta_1 \sin^2 \alpha. \quad (15)$$

As shown in Appendix A, the moveout approximation in equation 14 can be alternatively derived from generalized quartic coefficients in weakly anisotropic media on the basis of the perturbation theory in combination with the normalization factor in equation 12.

Analogously to the 2D case, we refer to the proposed approximation (equations 1 and 3) as generalized because of its ability to relate to several other known forms.

GENERAL METHOD FOR PARAMETER DEFINITION

To define the parameters in equation 1, we propose to use information from the zero-offset ray and four far-offset rays along the

x - and y -axes, $x = y$ and $x = -y$. Following an analogy with the 2D scheme by Fomel and Stovas (2010), we derive some of the coefficient formulas as follows.

Zero-offset ray

The Taylor expansion of equation 1 around the zero offset

$$t^2(x, y) \approx t_0^2 + W(x, y) + \frac{A(x, y)}{2t_0^2} + \dots \quad (16)$$

allows for a direct evaluation of nine coefficients: t_0 , W_i , and A_i by matching equation 16 with the expansion of the exact traveltime in vector offset.

Finite-offset rays

Suppose that each independent i th ray corresponds to ray parameters P_{xi} and P_{yi} and arrives at offset X_i and Y_i with reflection traveltme T_i . The i index ranges from one to four and denotes the associated ray direction of the x - and y -axes, $x = y$ and $x = -y$, respectively. Substituting moveout approximation 1 into equations $t(X_1, 0) = T_1$ and $dt/dX_1 = P_{x1}$ and solving for B_1 and C_1 , we have, from the ray along the x -axis ($i = 1$) (Fomel and Stovas, 2010)

$$B_1 = \frac{t_0^2(W_1 X_1 - P_{x1} T_1)}{X_1(t_0^2 - T_1^2 + P_{x1} T_1 X_1)} + \frac{W_1 A_1 X_1^2}{T_1^2 - t_0^2 - W_1 X_1^2}, \quad (17)$$

$$C_1 = \frac{t_0^4(W_1 X_1 - P_{x1} T_1)^2}{X_1^2(t_0^2 - T_1^2 + P_{x1} T_1 X_1)^2} + \frac{2A_1 t_0^2}{t_0^2 - T_1^2 + W_1 X_1^2}. \quad (18)$$

Analogously, B_3 and C_5 can be found from solving equations $t(0, Y_2) = T_2$ and $dt/dY_2 = P_{y2}$, which is equivalent to replacing X_1 , P_{x1} , and W_1 with Y_2 , P_{y2} , and W_3 , respectively in equations 17 and 18. The remaining coefficients B_2 , C_2 , C_3 , and C_4 can be solved numerically from the four conditions given below:

$$\left. \frac{\partial t}{\partial y} \right|_{y=0, x=X_1} = P_{y1}, \quad (19)$$

Table 1. Normalized stiffness tensor coefficients (in km^2/s^2) from different anisotropic samples: transversely isotropic medium with horizontal symmetry axis (HTI) is from Al-Dajani and Tsvankin (1998), layer 1 is from Schoenberg and Helbig (1997), layer 2 is from Tsvankin (1997), and layer 3 is a modified sample based on the same fracture model as layer 1.

Sample	c_{11}	c_{22}	c_{33}	c_{44}	c_{55}	c_{66}	c_{12}	c_{23}	c_{13}
HTI	5.06	7.086	7.086	2	2.25	2.25	1.033	3.086	1.033
Layer 1	9	9.84	5.938	2	1.6	2.182	3.6	2.4	2.25
Layer 2	11.7	13.5	9	1.728	1.44	2.246	8.824	5.981	5.159
Layer 3	12.6	13.94	8.9125	2.5	2	2.182	2.7	3.425	3.15

$$\frac{\partial t}{\partial x} \Big|_{x=0, y=Y_2} = P_{x2}, \quad (20)$$

$$t(X_3, X_3) = t(Y_3, Y_3) = T_3, \quad (21)$$

$$t(X_4, -X_4) = t(-Y_4, Y_4) = T_4. \quad (22)$$

They represent the matchings of P_{y1} and P_{x2} along rays in the x - and y -directions and traveltimes T_3 and T_4 along rays in the $x = y$ and $x = -y$ directions. Provided with the above information from the zero-offset ray and four finite-offset rays, we can define parameters appearing in the proposed moveout approximation (equation 1) in a systematic manner.

ACCURACY TESTS

Homogeneous HTI layer

To test the accuracy of the proposed approximation, we first consider a single horizontal layer of a transversely isotropic medium with horizontal symmetry axis (HTI) over a flat reflector with the properties given in Table 1 and with thickness of 1 km. The accuracy comparison between different approximations is shown in Figure 1 with the true traveltime being computed from ray tracing. The reference rays for the generalized approximation (equation 1) were chosen in terms of different ray parameters P_{xi} and P_{yi} , which then gives X_i , Y_i , and T_i , needed to solve for approximation coefficients according to equations 17–22. In this example, the reference rays are associated with $P_{x1} = 0.4$ and $P_{y1} = 0.0$ along the x -axis, with $P_{x2} = 0.0$ and $P_{y2} = 0.338$ along the y -axis, with $P_{x3} = 0.2$ and $P_{y3} = 0.103$ along $x = y$, and with $P_{x4} = 0.2$ and $P_{y4} = -0.103$ along $x = -y$. The proposed approximation shows a smaller error than the previous approximations (Figure 1c).

Homogeneous orthorhombic layer

For a more complex anisotropic medium, we consider a single horizontal layer of an orthorhombic material (layer 1) with properties given in Table 1 with 1 km thickness over a flat reflector. The accuracy comparison between the different approximations is shown in Figure 2. The reference rays for the generalized approximation (equation 1) were shot at $P_{x1} = 0.283$ and $P_{y1} = 0.0$ along the x -axis, at $P_{x2} = 0.0$ and $P_{y2} = 0.271$ along the y -axis, at $P_{x3} = 0.2$ and $P_{y3} = 0.169$ along $x = y$, and at $P_{x4} = 0.2$ and $P_{y4} = -0.169$ along $x = -y$. Note that the approximation by Xu et al. (2005) is a simplified version of that by Al-Dajani et al. (1998) in this particular case, and therefore, it produces almost identical results with only a small difference (Figure 2b and 2c). The proposed approximation shows an error that is several orders of magnitude smaller than that of previous approximations (Figure 2d).

Homogeneous orthorhombic layer with azimuthal rotation

Figure 3 shows the relative error plots of several approximations in a similar homogeneous orthorhombic model as in the previous

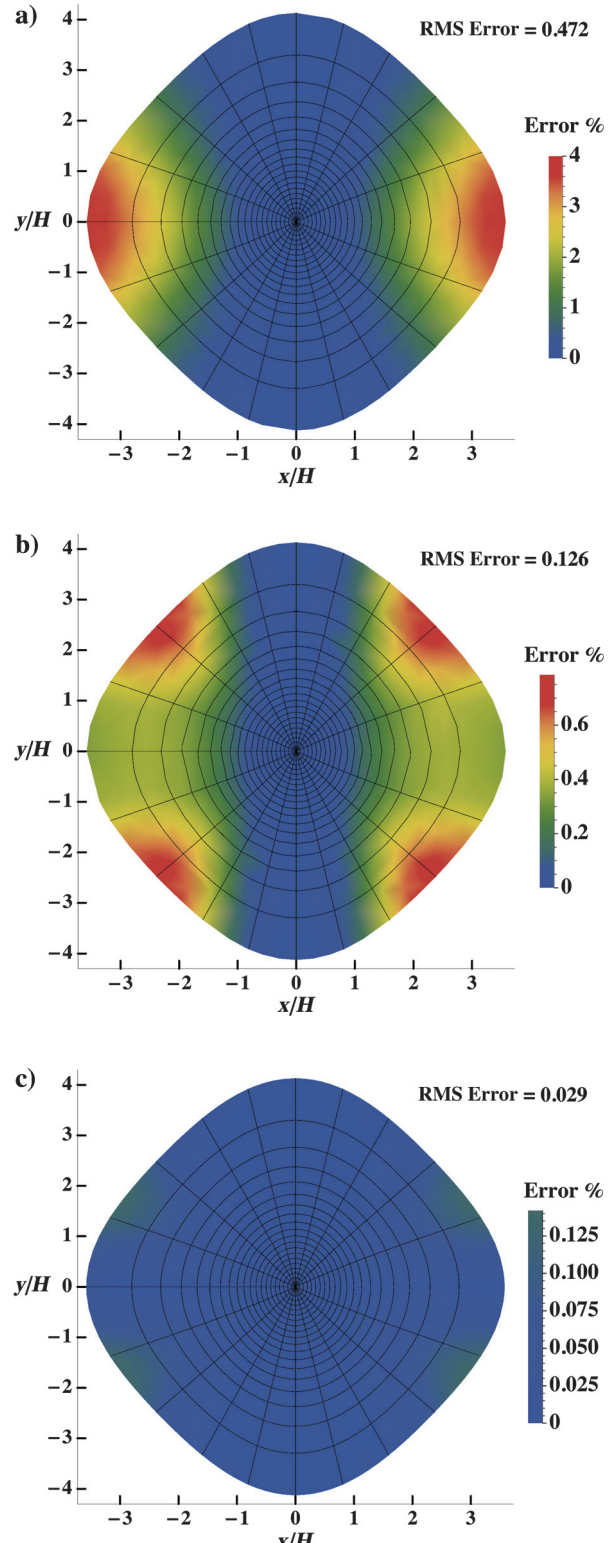


Figure 1. Error plots in the homogeneous HTI layer of the (a) NMO ellipse, (b) approximation by Al-Dajani and Tsvankin (1998) (similar to Al-Dajani et al., 1998), and (c) proposed approximation. Note that (b and c) are plotted under the same color scale and H denotes the reflector depth.

example, but with additional 30° azimuthal rotation with respect to the global coordinates. Assuming the rotation azimuth is known, the approximations by Al-Dajani et al. (1998) and Xu et al. (2005) behave largely similarly to the original case with the error plots rotated (Figure 3b and 3c). The proposed approximation is implemented based on the global coordinate system regardless of the azimuthal

orientation of the orthorhombic symmetry plane and leads to a significantly more accurate result (Figure 3d). The reference rays were shot at $P_{x1} = 0.289$ and $P_{y1} = 0.004$ along the x -axis, at $P_{x2} = 0.032$ and $P_{y2} = 0.282$ along the y -axis, at $P_{x3} = 0.2$ and $P_{y3} = 0.206$ along $x = y$, and at $P_{x4} = 0.2$ and $P_{y4} = -0.163$ along $x = -y$.

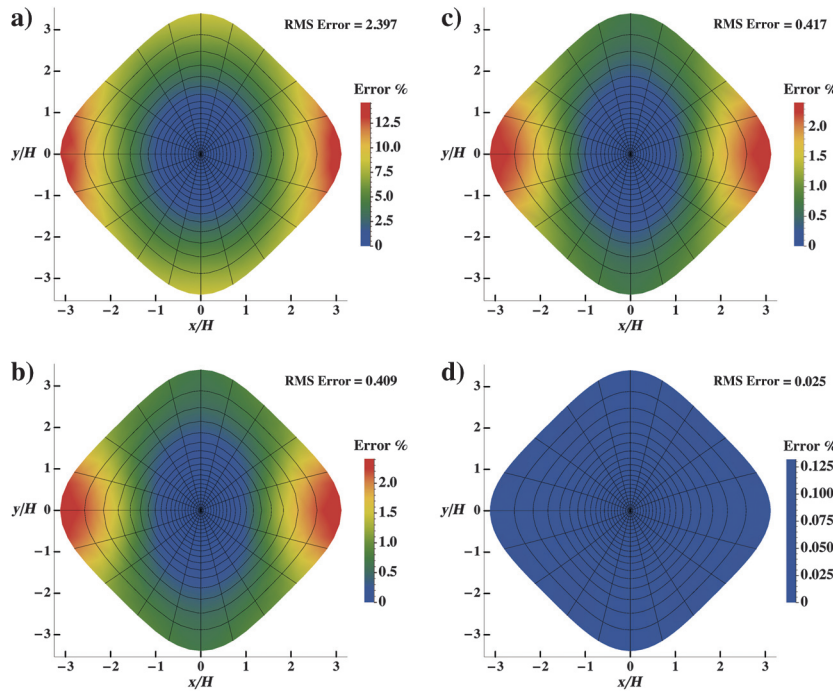


Figure 2. Error plots in the homogeneous orthorhombic layer (layer 1) of the (a) NMO ellipse, (b) approximation by Al-Dajani et al. (1998), (c) approximation by Xu et al. (2005), and (d) proposed approximation. Note that (b-d) are plotted under the same color scale and H denotes the reflector depth.

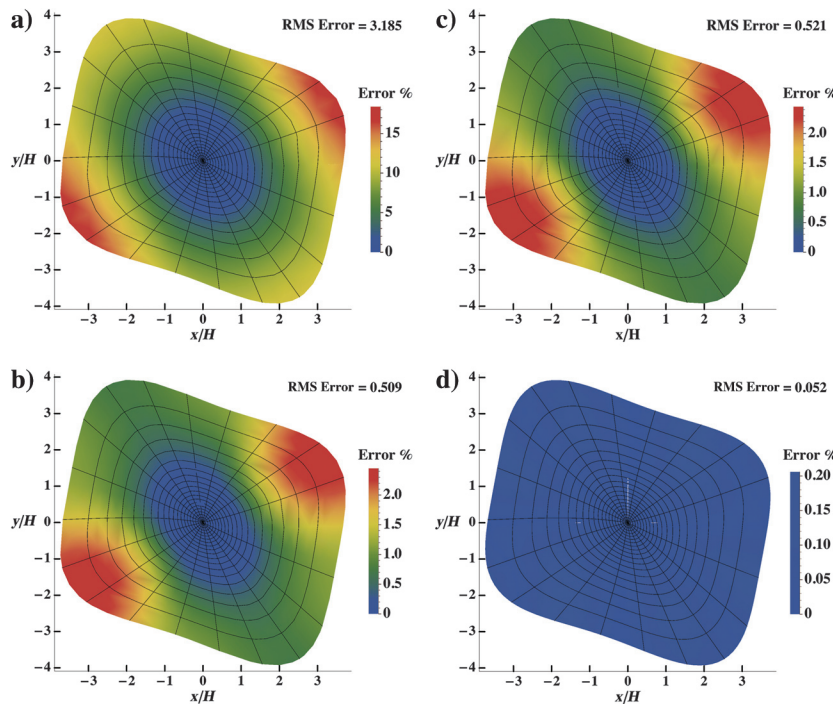


Figure 3. Error plots in the 30° rotated homogeneous orthorhombic layer (layer 1) of the (a) NMO ellipse, (b) approximation by Al-Dajani et al. (1998), (c) approximation by Xu et al. (2005), and (d) proposed approximation. Note that (b-d) are plotted under the same color scale and H denotes the reflector depth.

Layered orthorhombic model

We also test the accuracy of the proposed approximation in a three-layer orthorhombic model over a flat reflector with the parameters (layers 1–3) listed in Table 1. The thicknesses of the three layers are 0.25, 0.45, and 0.3 km, respectively. For previously pro-

posed approximations, the effective coefficients are calculated, as the original authors suggested, by the VTI averaging relationship (Hake et al., 1984; Tsvankin and Thomsen, 1994). The reference rays for the proposed approximation (equation 1) were shot at $P_{x1} = 0.254$ and $P_{y1} = 0.0$ along the x -axis, at $P_{x2} = 0$ and $P_{y2} = 0.24$ along the y -axis, at $P_{x3} = 0.195$ and $P_{y3} = 0.166$ along $x = y$,

Figure 4. Error plots in the aligned three-layer orthorhombic model of the (a) NMO ellipse, (b) approximation by Al-Dajani et al. (1998), (c) approximation by Xu et al. (2005), and (d) proposed approximation. Note that (b-d) are plotted under the same color scale and H denotes the reflector depth.

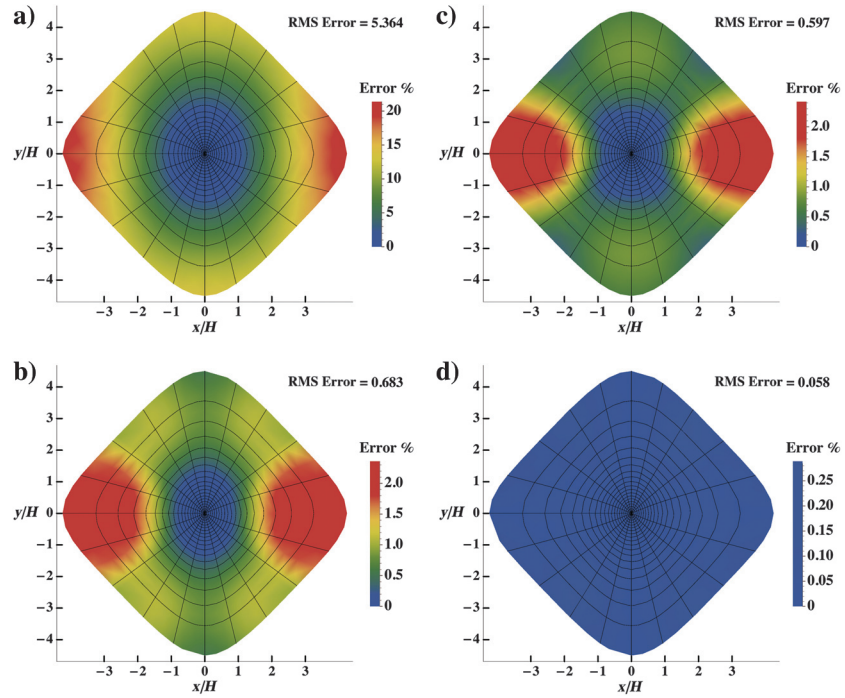
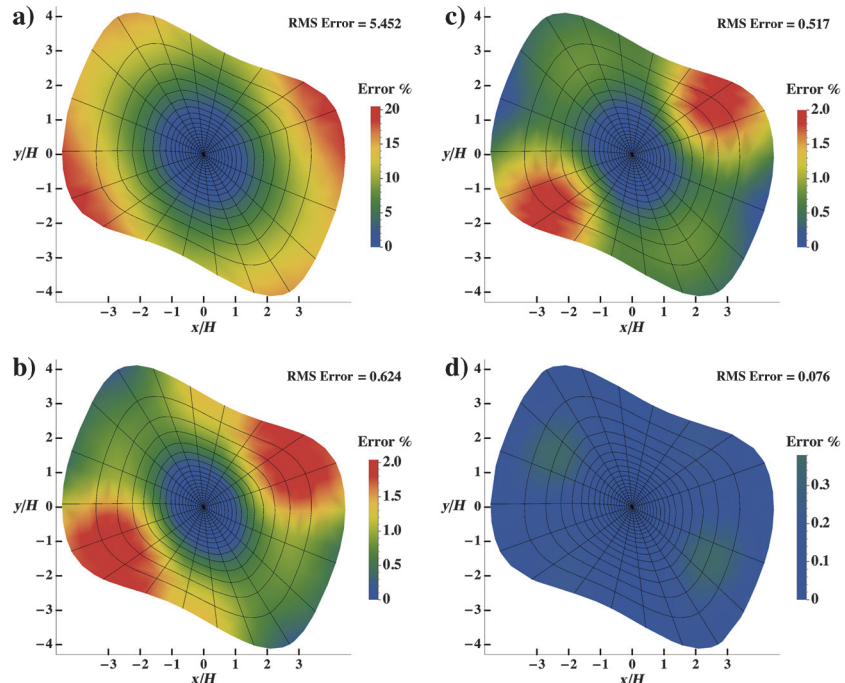


Figure 5. Error plots in the three-layer orthorhombic model with azimuthal rotation of sublayers (50° in the middle layer and 30° in the bottom layer) of the (a) NMO ellipse, (b) approximation by Al-Dajani et al. (1998), (c) approximation by Xu et al. (2005), and (d) the proposed approximation. Note that (b-d) are plotted under the same color scale and H denotes the reflector depth.



and at $P_{x4} = 0.21$ and $P_{y4} = -0.182$ along $x = -y$. The proposed generalized approximation performs with the highest accuracy (Figure 4).

Layered orthorhombic model with azimuthal rotation in sublayers

For a more complex model, we introduce azimuthal rotation of 50° and 30° in the middle layer (layer 2) and the bottom layer (layer 3) of the three-layer model from the previous example, respectively. The angle measurement is done with respect to the top layer. Similarly to before, the effective coefficients for previously proposed approximations are calculated by the VTI averaging relationship. The reference rays for the proposed approximation (equation 1) are shot at $P_{x1} = 0.254$ and $P_{y1} = 0.005$ along the x -axis, at $P_{x2} = 0.029$ and $P_{y2} = 0.24$ along the y -axis, at $P_{x3} = 0.18$ and $P_{y3} = 0.198$ along $x = y$, and at $P_{x4} = 0.2$ and $P_{y4} = -0.184$ along $x = -y$. The proposed generalized approximation again shows the highest accuracy (Figure 5).

Layered orthorhombic model from SEAM Phase II unconventional model

For a complex numerical test, we create a 1D layered orthorhombic model (Figure 6) by extracting a depth column out of the SEAM Phase II unconventional model (Oristaglio, 2015). We assume no azimuthal rotation in the sublayers. Therefore, this model represents an example of a complex layered orthorhombic model with aligned symmetry planes. The reflection traveltimes and offsets can be computed from ray tracing and are shown in Figure 7. Note that because this is a layered orthorhombic medium with aligned symmetry planes, it is sufficient to show the results only in one quadrant defined by the two slowness components p_x and p_y as they remain symmetric in all other possible quadrants. Following the similar process as in previous examples, Figure 8 shows a performance comparison of various moveout approximations. The reference rays for the proposed GMA (equation 1) are shot at $P_{x1} = 0.124$ and $P_{y1} = 0.0$ along the x -axis, at $P_{x2} = 0.0$ and $P_{y2} = 0.133$ along the y -axis, at $P_{x3} = 0.084$ and $P_{y3} = 0.0983$ along $x = y$, and at $P_{x4} = 0.085$ and $P_{y4} = -0.0996$ along $x = -y$. The proposed generalized approximation shows again the highest accuracy with the maximum travelttime error of 6.66 ms and root-mean-square (rms) error of 0.083 ms. The maximum travelttime and rms errors for the other approximations are 309.75 and 18.86 ms for the NMO ellipse, 66.33 and 2.975 ms for the approximation by Al-Dajani et al.

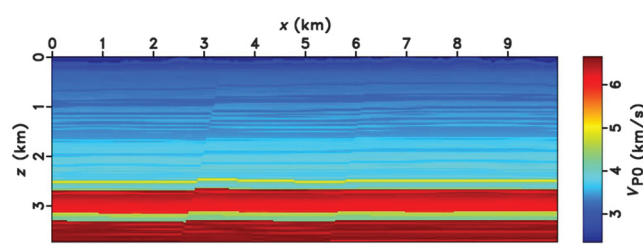


Figure 6. Vertical P-wave velocity in kilometers per second of the SEAM Phase II unconventional model.

(1998), and 110.87 and 3.829 ms for the approximation by Xu et al. (2005).

DISCUSSION

The choice of scheme for defining the coefficient parameters can have an effect on the approximation accuracy. We chose to fit nine parameters (t_0 , W_i , and A_i) along the zero-offset ray. The remaining eight parameters are divided into six and two fitting equations. The former is from T_1 , P_{x1} , and P_{y1} along the x -axis and T_2 , P_{x2} , and P_{y2} along the y -axis, whereas the latter is from T_3 and T_4 along $x = y$ and $x = -y$. Another possible option is to consider T_i and the radial ray parameter $P_{ri}(P_{xi}, P_{yi})$, which would allow two fitting equations from all four directions and make the fitting scheme more symmetric. However, this approach degenerates even in the simple

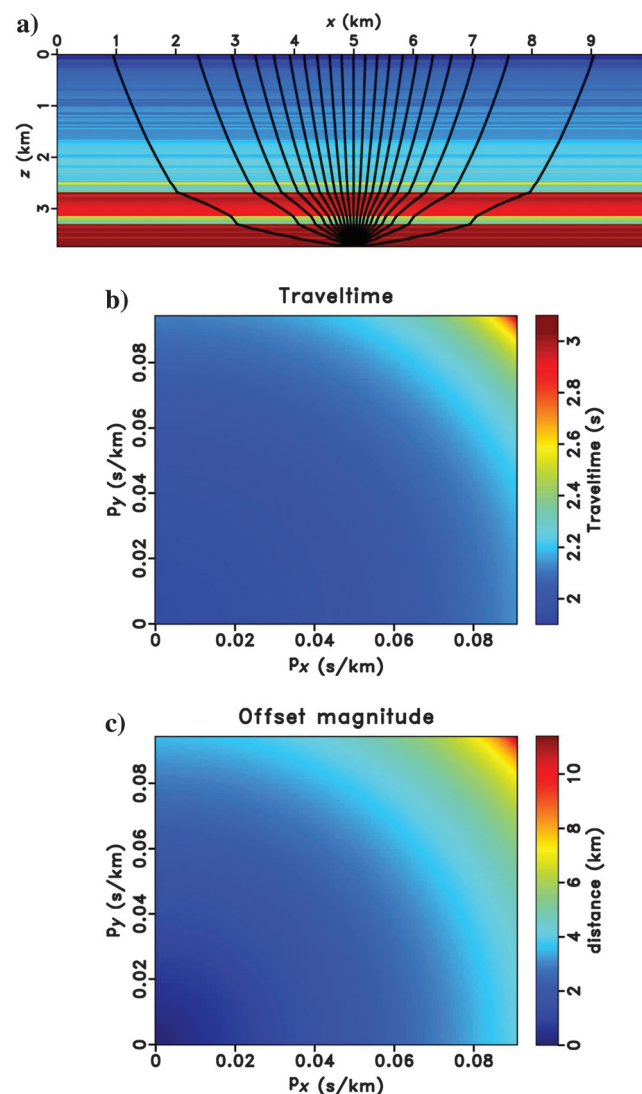


Figure 7. The 1D model construct from the first column of SEAM Phase II unconventional model and (a) example reflection rays at constant $p_x = 0.0908$ and varying p_y from 0 to 0.09425. The exact travelttime and the magnitude of offset $r = \sqrt{x^2 + y^2}$ are shown in (b and c) for increasing values of slowness components p_x and p_y .

case of a homogeneous orthorhombic layer due to the similarity between $x = y$ and $x = -y$ directions caused by the orthorhombic symmetry. Therefore, we do not propose to use such a scheme.

Moreover, the selection of particular rays shot according to the proposed scheme also influences the accuracy level. This issue is originally pointed out by Fomel and Stovas (2010), and is addressed by Hao and Stovas (2014) in the case of 3D HTI media. In our experiments, we observe that given the four rays at sufficiently far offsets, one can expect the proposed approximation to perform with sufficiently high accuracy for practical purposes with smaller errors closer to the chosen reference offsets.

Analogously to the 2D GMA of Fomel and Stovas (2010), the proposed approximation assumes that the traveltime at an infinite offset behaves quadratically as

$$t^2(x, y) \approx T_\infty^2 + P_{x_\infty}^2 x^2 + P_{xy_\infty}^2 xy + P_{y_\infty}^2 y^2, \quad (23)$$

and there are no linear terms present. This might introduce some errors in a special case of having an anomalously high-velocity sublayer in a layered medium (Blas, 2013; Ravve and Koren, 2016). In our approximation, we choose not to complicate the functional form by introducing more parameters to deal with this issue.

Even though the required number of parameters for the proposed approximation (17) is high, this number is necessary for an accurate handling of anisotropy with complication from the possible azimuthal rotation of the subsurface in 3D. Although other previously proposed approximations require fewer parameters, they may not produce equally accurate results. Figure 9 shows the results approximation of Xu et al. (2005) for the two models from the last section, when a 20% error is introduced in the known azimuthal rotation. We can observe a significant decrease in accuracy especially in the layered case.

In the case of a single orthorhombic layer, the moveout approximation proposed in our earlier work (Sripanich and Fomel, 2015b),

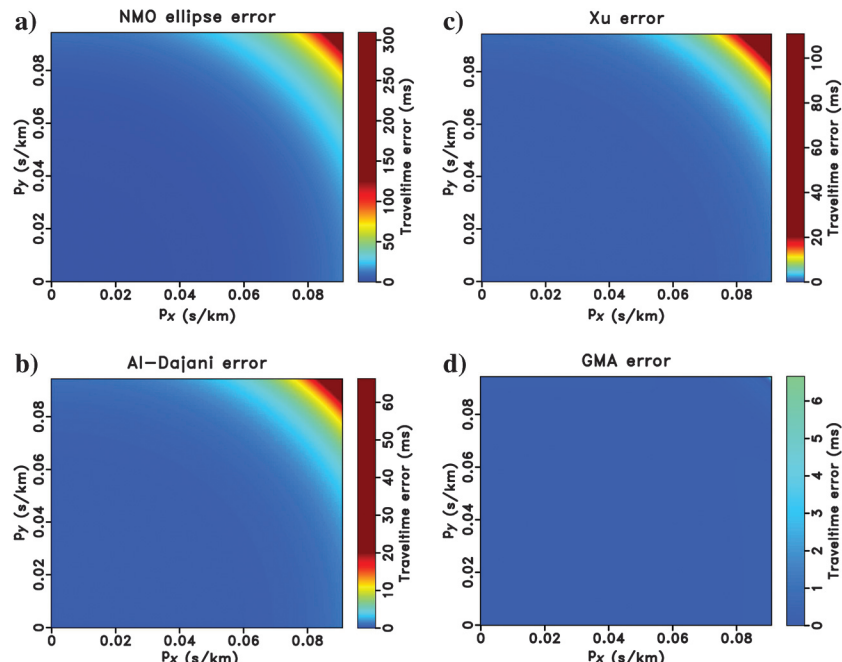
Figure 8. Error plots in the 1D layered orthorhombic model form of SEAM Phase II unconventional model: the (a) NMO ellipse, (b) approximation by Al-Dajani et al. (1998), (c) approximation by Xu et al. (2005), and (d) proposed approximation. Note that (a) is plotted with 120 ms clipping, whereas (b-d) are plotted under the same color scale with 25 ms clipping. The scale bars show the total range of errors for different approximations. The proposed approximation achieves the highest accuracy with the maximum traveltime error of 6.66 ms and rms error of 0.083 ms.

while requiring only six parameters, exhibits the same level of accuracy as the generalized approximation (Figure 10a). This indicates that the additional nonzero parameters in equation 1 can be captured by the relationship between anelliptic parameters in each symmetry plane (Sripanich and Fomel, 2015b; Sripanich et al., 2016). However, this approach may not be sufficiently accurate in a layered model (Figure 10b).

Provided that a reflection event can be accurately defined in a gather, the proposed 3D moveout approximation is suitable for anisotropic parameter estimation. One possible method for this application to real seismic data is time warping (Burnett and Fomel, 2009; Casasanta, 2011; Casasanta and Fomel, 2011), which uses overdetermined least-squares parameter inversion based on local slope estimation and nonphysical flattening by predictive painting (Fomel, 2010). This method enables, in principle, an estimation of all 17 effective parameters in equation 1, which can then be inverted for interval values in a layer-stripping fashion (Sripanich and Fomel, 2016). In the presence of lateral heterogeneity, the results from such global inversion can be used as an initial model for more sophisticated inversion techniques.

CONCLUSION

We have introduced an extension of the GMA to 3D. The proposed approximation, similarly to its 2D analog, reduces to several known functional forms with particular choices of parameters. The approximation requires 17 parameters, which are uniquely defined by zero-offset computations and four additional finite-offset rays. Our numerical tests show that, in comparison with other known 3D moveout approximations, the proposed approximation produces results with superior accuracy, which is not surprising given the larger number of adjustable parameters. Its advantage becomes more obvious with more complex models. Moreover, the proposed approximation performs well even in the presence of anisotropic



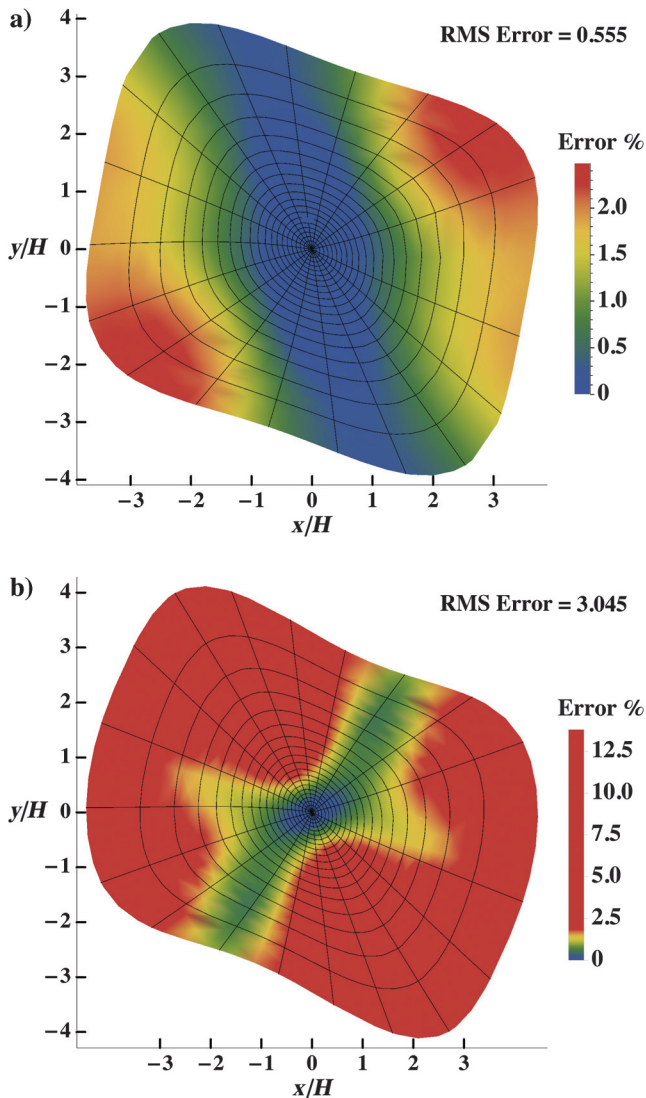


Figure 9. Error plots of the approximation by Xu et al. (2005) in (a) the rotated homogeneous orthorhombic layer (layer 1) and (b) the three-layer orthorhombic model with azimuthal rotation in sublayers plotted under similar color scales as the originals when 20% error is introduced in known azimuthal angles. One can observe significantly higher errors compared with the original ones in Figures 3c and 5c.

axis rotation and multiple layers, suggesting that only 17 parameters are sufficient to describe the reflection traveltimes in a model with 3D anisotropic layers. In our experiments, the accuracy can be nearly exact for practical purposes with less than 0.3% of maximum error in the homogeneous and complex layered anisotropic models. The proposed moveout approximation can be readily used for forward reflection traveltimes computation or as a basis for inversion for anisotropic parameters from seismic reflection data.

ACKNOWLEDGMENTS

We thank the assistant editor, J. Etgen, the associate editor, and three anonymous reviewers for their constructive comments. We

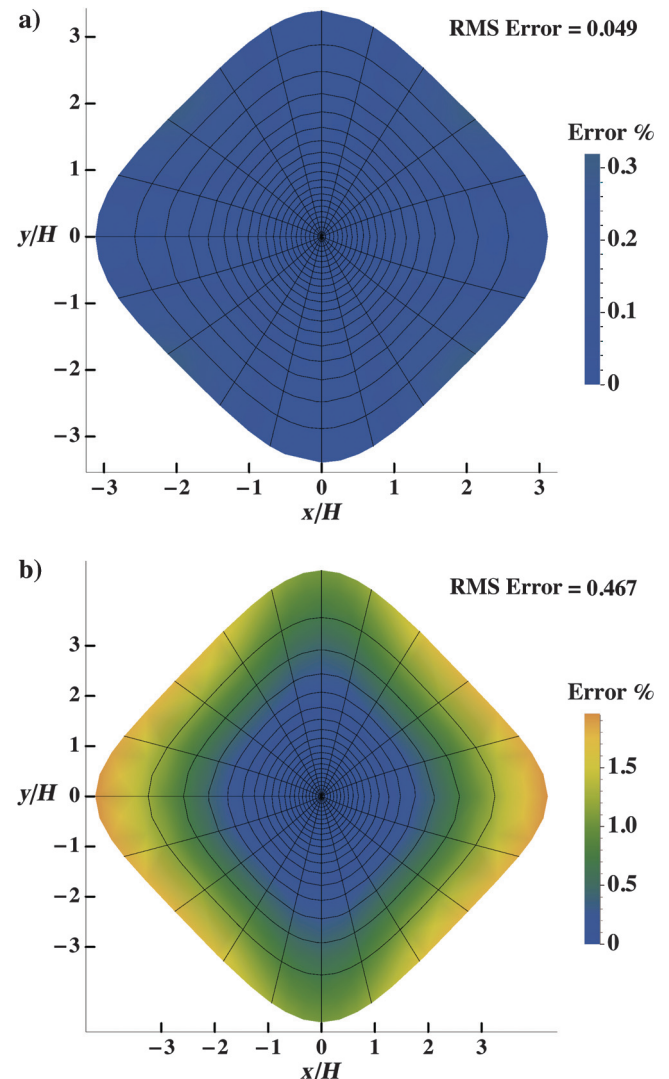


Figure 10. Error plots of the approximation by Sripanich and Fomel (2015b) in (a) the homogeneous orthorhombic layer (layer 1) and (b) the aligned three-layer orthorhombic model.

thank the sponsors of the Texas Consortium for Computational Seismology and the Rock Seismic Research Project for financial support. Y. Sripanich is also grateful to the additional support by the Statoil Fellows Program at the University of Texas at Austin. We are grateful to the Exploration Development Geophysics Education and Research and BP America for their permission to use SEAM Phase II unconventional model in this study.

APPENDIX A ALTERNATIVE DERIVATION OF THE MOVEOUT APPROXIMATION IN EQUATION 14

On the basis of perturbation theory for a general horizontal homogeneous weakly anisotropic media, we consider the quartic coefficients in equations 1 and 3, A_i , to be (Grechka and Pech, 2006; Farra et al., 2016)

$$\begin{aligned} A_1 &= -\frac{4\eta_2}{V_{\text{ref}}^4}, \quad A_2 = \frac{8(\chi_{13} - \chi_{11})}{V_{\text{ref}}^4}, \\ A_3 &= -\frac{4(\eta_1 + \eta_2 - \eta_3)}{V_{\text{ref}}^4}, \quad A_4 = \frac{8(\chi_{13} - \chi_{12})}{V_{\text{ref}}^4}, \quad \text{and} \\ A_5 &= -\frac{4\eta_1}{V_{\text{ref}}^4}, \end{aligned} \quad (\text{A-1})$$

where

$$\chi_{11} = \frac{c_{16}}{V_{\text{ref}}}, \quad \chi_{12} = \frac{c_{26}}{V_{\text{ref}}}, \quad \chi_{13} = \frac{c_{36} + 2c_{45}}{V_{\text{ref}}}, \quad (\text{A-2})$$

and V_{ref} denotes the P-wave velocity in the chosen isotropic background. These expressions are appropriate for horizontal homogeneous weakly anisotropic media of any symmetry. A more general form for a dipping layer is also discussed by Grechka and Pech (2006). In the specific case of orthorhombic media, the general quartic coefficients (equation A-1) can be simplified to

$$A_r(\alpha) = -\frac{4\eta(\alpha)}{V_{\text{ref}}^4}, \quad (\text{A-3})$$

where $\eta(\alpha)$ is given in equation 15. Therefore, the resulting moveout approximation takes the form of

$$t^2(r, \alpha) \approx t_0^2 + W_r(\alpha)r^2 - \frac{2\eta(\alpha)}{t_0^2 V_{\text{ref}}^4} r^4. \quad (\text{A-4})$$

Subsequently, by setting

$$V_{\text{ref}}^2 = V_{\text{NMO}}^2(\alpha) = (W_r(\alpha))^{-1}, \quad (\text{A-5})$$

we obtain the moveout approximation of the form proposed by Xu et al. (2005) and Vasconcelos and Tsvankin (2006):

$$t^2(r, \alpha) \approx t_0^2 + W_r(\alpha)r^2 - \frac{2\eta(\alpha)}{t_0^2 V_{\text{NMO}}^2(\alpha)} r^4, \quad (\text{A-6})$$

without the long-offset normalization, which corresponds to the choice of $A_r(\alpha) = -4\eta(\alpha)/V_{\text{NMO}}^4(\alpha)$, $B_i = 0$, and $C_i = 0$ from equation 3. The additional long-offset normalization factor can be included based on the same scheme as in equation 12 with

$$A_r^*(\alpha) = \frac{1 + 2\eta(\alpha)}{t_0^2 V_{\text{NMO}}^2(\alpha)}. \quad (\text{A-7})$$

As a result, we obtain the same expression of the moveout approximation in equation 14 by Xu et al. (2005) in the main text.

REFERENCES

- Al-Dajani, A., and I. Tsvankin, 1998, Nonhyperbolic reflection moveout for horizontal transverse isotropy: Geophysics, **63**, 1738–1753, doi: [10.1190/1.1444469](https://doi.org/10.1190/1.1444469).
- Al-Dajani, A., I. Tsvankin, and M. N. Toksöz, 1998, Non-hyperbolic reflection moveout for azimuthally anisotropic media: 68th Annual International Meeting, SEG, Expanded Abstracts, 1479–1482.
- Aleixo, R., and J. Schleicher, 2010, Traveltime approximations for qP waves in vertical transversely isotropic media: Geophysical Prospecting, **58**, 191–201, doi: [10.1111/j.1365-2478.2009.00815.x](https://doi.org/10.1111/j.1365-2478.2009.00815.x).
- Alkhalifah, T., 1998, Acoustic approximations for processing in transversely isotropic media: Geophysics, **63**, 623–631, doi: [10.1190/1.1444361](https://doi.org/10.1190/1.1444361).
- Alkhalifah, T., 2003, An acoustic wave equation for orthorhombic anisotropy: Geophysics, **68**, 1169–1172, doi: [10.1190/1.1598109](https://doi.org/10.1190/1.1598109).
- Alkhalifah, T., and I. Tsvankin, 1995, Velocity analysis for transversely isotropic media: Geophysics, **60**, 1550–1566, doi: [10.1190/1.1443888](https://doi.org/10.1190/1.1443888).
- Blas, E., 2009, Long-offset NMO approximation for a layered VTI model: Model study: 79th Annual International Meeting, SEG, Expanded Abstracts, 3745–3748.
- Blas, E., 2013, High-accuracy two-interval approximation for normal-moveout function in a multi-layered anisotropic model: Geophysical Prospecting, **61**, 1229–1237, doi: [10.1111/1365-2478.12059](https://doi.org/10.1111/1365-2478.12059).
- Burnett, W., and S. Fomel, 2009, Moveout analysis by time-warping: 79th Annual International Meeting, SEG, Expanded Abstracts, 3710–3714.
- Casasanta, L., 2011, NMO-ellipse independent 3D moveout analysis in τ - p domain: 81st Annual International Meeting, SEG, Expanded Abstracts, 289–294.
- Casasanta, L., and S. Fomel, 2011, Velocity-independent τ - p moveout in a horizontally-layered VTI medium: Geophysics, **76**, no. 4, U45–U57, doi: [10.1190/1.3595776](https://doi.org/10.1190/1.3595776).
- Castle, R. J., 1994, Theory of normal moveout: Geophysics, **59**, 983–999, doi: [10.1190/1.1443658](https://doi.org/10.1190/1.1443658).
- Farra, V., I. Pšenčík, and P. Jílek, 2016, Weak-anisotropy moveout approximations for P-waves in homogeneous layers of monoclinic or higher anisotropy symmetries: Geophysics, **81**, no. 2, C17–C37, doi: [10.1190/geo2015-0223.1](https://doi.org/10.1190/geo2015-0223.1).
- Fomel, S., 1994, Recurrent formulas for derivatives of a CDP travel-time curve: Russian Geology and Geophysics, **35**, 118–126.
- Fomel, S., 2004, On anelliptic approximations for qP velocities in VTI media: Geophysical Prospecting, **52**, 247–259, doi: [10.1111/j.1365-2478.2004.00413.x](https://doi.org/10.1111/j.1365-2478.2004.00413.x).
- Fomel, S., 2010, Predictive painting of 3-D seismic volumes: Geophysics, **75**, no. 4, A25–A30, doi: [10.1190/1.3453847](https://doi.org/10.1190/1.3453847).
- Fomel, S., and V. Grechka, 2001, Nonhyperbolic reflection moveout of P-waves: An overview and comparison of reasons: Center for Wave Phenomena, CWP-372.
- Fomel, S., and A. Stovas, 2010, Generalized nonhyperbolic moveout approximation: Geophysics, **75**, no. 2, U9–U18, doi: [10.1190/1.3334323](https://doi.org/10.1190/1.3334323).
- Golikov, P., and A. Stovas, 2012, Accuracy comparison of nonhyperbolic moveout approximations for qP-waves in VTI media: Journal of Geophysics and Engineering, **9**, 428–432, doi: [10.1088/1742-2132/9/4/428](https://doi.org/10.1088/1742-2132/9/4/428).
- Grechka, V., and A. Pech, 2006, Quartic reflection moveout in a weakly anisotropic dipping layer: Geophysics, **71**, no. 1, D1–D13, doi: [10.1190/1.2159047](https://doi.org/10.1190/1.2159047).
- Grechka, V., and I. Tsvankin, 1998, 3-D description of normal moveout in anisotropic inhomogeneous media: Geophysics, **63**, 1079–1092, doi: [10.1190/1.1444386](https://doi.org/10.1190/1.1444386).
- Hake, H., K. Helbig, and C. S. Mesdag, 1984, Three-term Taylor series for t^2 - x^2 curves over layered transversely isotropic ground: Geophysical Prospecting, **32**, 828–850, doi: [10.1111/j.1365-2478.1984.tb00742.x](https://doi.org/10.1111/j.1365-2478.1984.tb00742.x).
- Hao, Q., and A. Stovas, 2014, Three dimensional generalized nonhyperbolic moveout approximation: Application on a 3D HTI model: 76th Annual International Conference and Exhibition, EAGE, Extended Abstracts, 665–668, doi: [10.3997/2214-4609.20140868](https://doi.org/10.3997/2214-4609.20140868).
- Hao, Q., and A. Stovas, 2015, Generalized moveout approximation for P-SV converted waves in vertically inhomogeneous transversely isotropic media with a vertical symmetry axis: Geophysical Prospecting, **64**, 1469–1482, doi: [10.1111/1365-2478.12353](https://doi.org/10.1111/1365-2478.12353).
- Oristaglio, M., 2015, Elastic anisotropy in SEAM Phase II models: The Leading Edge, **34**, 964–970, doi: [10.1190/tle34080964.1](https://doi.org/10.1190/tle34080964.1).
- Pech, A., V. Grechka, and I. Tsvankin, 2003, Quartic moveout coefficient: 3D description and application to tilted TI media: Geophysics, **68**, 1600–1610, doi: [10.1190/1.1620634](https://doi.org/10.1190/1.1620634).
- Pech, A., and I. Tsvankin, 2004, Quartic moveout coefficient for a dipping azimuthally anisotropic layer: Geophysics, **69**, 699–707, doi: [10.1190/1.1759456](https://doi.org/10.1190/1.1759456).
- Ravve, I., and Z. Koren, 2016, Long-offset moveout approximation for VTI elastic layered media: 78th Annual International Conference and Exhibition, EAGE, Extended Abstracts, doi: [10.3997/2214-4609.201600732](https://doi.org/10.3997/2214-4609.201600732).
- Schoenberg, M., and K. Helbig, 1997, Orthorhombic media: Modeling elastic wave behavior in a vertically fractured earth: Geophysics, **62**, 1954–1974, doi: [10.1190/1.1444297](https://doi.org/10.1190/1.1444297).
- Sripanich, Y., and S. Fomel, 2015a, 3D generalized nonhyperboloidal moveout approximation: 85th Annual International Meeting, SEG, Expanded Abstracts, 5147–5152.
- Sripanich, Y., and S. Fomel, 2015b, On anelliptic approximations for qP velocities in transversely isotropic and orthorhombic media: Geophysics, **80**, no. 5, C89–C105, doi: [10.1190/geo2014-0534.1](https://doi.org/10.1190/geo2014-0534.1).

- Sripnich, Y., and S. Fomel, 2016, Theory of interval parameter estimation in layered anisotropic media: *Geophysics*, **81**, no. 5, C253–C263, doi: [10.1190/geo2016-0013.1](https://doi.org/10.1190/geo2016-0013.1).
- Sripnich, Y., S. Fomel, P. Fowler, A. Stovas, and K. Spikes, 2016, Muir-dellinger parameters for analysis of anisotropic signatures: Presented at the 17th International Workshop on Seismic Anisotropy (IWSA).
- Stovas, A., 2010, Generalized moveout approximation for qP-and qSV-waves in a homogeneous transversely isotropic medium: *Geophysics*, **75**, no. 6, D79–D84, doi: [10.1190/1.3506504](https://doi.org/10.1190/1.3506504).
- Stovas, A., 2015, Azimuthally dependent kinematic properties of orthorhombic media: *Geophysics*, **80**, no. 6, C107–C122, doi: [10.1190/geo2015-0288.1](https://doi.org/10.1190/geo2015-0288.1).
- Stovas, A., and S. Fomel, 2012, Generalized nonelliptic moveout approximation in τ - p domain: *Geophysics*, **77**, no. 2, U23–U30, doi: [10.1190/geo2011-0119.1](https://doi.org/10.1190/geo2011-0119.1).
- Taner, M. T., S. Treitel, and M. Al-Chalabi, 2005, A new traveltine estimation method for horizontal strata: 75th Annual International Meeting, SEG, Expanded Abstracts, 2273–2276.
- Thomsen, L., 2014, Understanding seismic anisotropy in exploration and exploitation (2nd ed.): SEG and EAGE.
- Tsvankin, I., 1997, Anisotropic parameters and P-wave velocity for orthorhombic media: *Geophysics*, **62**, 1292–1309, doi: [10.1190/1.1444231](https://doi.org/10.1190/1.1444231).
- Tsvankin, I., and V. Grechka, 2011, Seismology of azimuthally anisotropic media and seismic fracture characterization: SEG.
- Tsvankin, I., and L. Thomsen, 1994, Non-hyperbolic reflection moveout in anisotropic media: *Geophysics*, **59**, 1290–1304, doi: [10.1190/1.1443686](https://doi.org/10.1190/1.1443686).
- Ursin, B., and A. Stovas, 2006, Traveltine approximations for a layered transversely isotropic medium: *Geophysics*, **71**, no. 2, D23–D33, doi: [10.1190/1.2187716](https://doi.org/10.1190/1.2187716).
- Vasconcelos, I., and I. Tsvankin, 2006, Non-hyperbolic moveout inversion of wide-azimuth P-wave data for orthorhombic media: *Geophysical Prospecting*, **54**, 535–552, doi: [10.1111/j.1365-2478.2006.00559.x](https://doi.org/10.1111/j.1365-2478.2006.00559.x).
- Xu, X., I. Tsvankin, and A. Pech, 2005, Geometrical spreading of P-waves in horizontally layered, azimuthally anisotropic media: *Geophysics*, **70**, no. 5, D43–D53, doi: [10.1190/1.2052467](https://doi.org/10.1190/1.2052467).
- Yilmaz, O., 2001, Seismic data analysis (2nd ed.): SEG.